The role of membrane-bound metal ions in toxicity of a human cancer cell-active pore-forming toxin Cry41Aa from Bacillus thuringiensis

Article (Accepted Version)

Accepted Manuscript

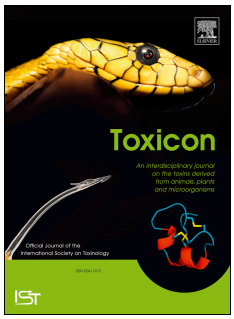

The role of membrane-bound metal ions in toxicity of a human cancer cell-active pore-forming toxin Cry41Aa from *Bacillus thuringiensis*

Barbara Domanska, Eva Fortea, Michelle J. West, Jean-Louis Schwartz, Neil Crickmore

PII: S0041-0101(19)30170-9

DOI: https://doi.org/10.1016/j.toxicon.2019.06.003

Reference: TOXCON 6142

To appear in: *Toxicon*

Received Date: 4 March 2019

Revised Date: 9 May 2019

Accepted Date: 3 June 2019

Please cite this article as: Domanska, B., Fortea, E., West, M.J., Schwartz, J.-L., Crickmore, N., The role of membrane-bound metal ions in toxicity of a human cancer cell-active pore-forming toxin Cry41Aa from *Bacillus thuringiensis*, *Toxicon* (2019), doi: https://doi.org/10.1016/j.toxicon.2019.06.003.

The role of membrane-bound metal ions in toxicity of a human cancer cell-active pore-forming toxin Cry41Aa from *Bacillus thuringiensis*

Barbara Domanska[1#], Eva Fortea[2, 3], Michelle J. West[1], Jean-Louis Schwartz[2] and Neil Crickmore[1]

[1] School of Life Sciences, University of Sussex, Falmer, Brighton BN1 9QG, UK.

[2] Département de pharmacologie et physiologie, Université de Montréal, Montréal, Québec, H3C 3J7, Canada.

[3] Cornell Graduate School of Medical Sciences, 1300 York Avenue, New York, NY 10065, USA.

[#] Corresponding author: Barbara Domanska, B.Domanska@sussex.ac.uk

Abstract

Bacillus thuringiensis crystal (Cry) proteins, used for decades as insecticidal toxins, are well known to be toxic to certain insects, but not to mammals. A novel group of Cry toxins called parasporins possess a strong cytocidal activity against some human cancer cells. Cry41Aa, or parasporin3, closely resembles commercially used insecticidal toxins and yet is toxic to the human hepatic cancer cell line HepG2, disrupting membranes of susceptible cells, similar to its insecticidal counterparts. In this study, we explore the protective effect that the common divalent metal chelator EGTA exerts on Cry41Aa's activity on HepG2 cells. Our results indicate that rather than interfering with a signalling pathway as a result of chelating cations in the medium, the chelator prevented the toxin's interaction with the membrane, and thus the subsequent steps of membrane damage and p38 phosphorylation, by removing cations bound to plasma membrane components. BAPTA and DTPA also inhibited Cry41Aa toxicity but at higher concentrations. We also show for the first time that Cry41Aa induces pore formation in planar lipid bilayers. This activity is not altered by EGTA, consistent with a biological context of chelation. Salt supplementation assays identified Ca^{2+}, Mn^{2+} and Zn^{2+} as being able to reinstate Cry41Aa activity. Our data suggest the existence of one or more metal cation-dependent receptors in the Cry41Aa mechanism of action.

Keywords: EGTA · Parasporin · Pore-forming toxin · HepG2 · Cry toxin · Planar lipid bilayers · Patch-clamping

Abbreviations: EGTA, ethylene glycol-bis(β-aminoethyl ether)-N,N,N',N'-tetraacetic acid; EDTA, 2, 2', 2'', 2''' -(Ethane-1, 2-diyldinitrilo) tetraacetic acid; BAPTA, 1,2-bis(o-aminophenoxy)ethane-N,N,N′,N′-tetraacetic acid; DTPA, 2-[Bis[2-[bis(carboxymethyl)amino]ethyl]amino]acetic acid; BBMV, brush border membrane vesicles;POPC, 1palmitoyl-2-oleoyl-sn-glycero-3phosphocholine; POPE, 1-palmitoyl-2oleoyl-sn-glycero-3-phosphoethanolamine.

1. Introduction

Bacillus thuringiensis (*Bt*) is an entomopathogenic bacterium that, among other virulence factors, produces parasporal crystal (Cry) proteins used commercially as insecticides in sprays and expressed in transgenic crops (1). After solubilisation and proteolytic activation in the insect gut, they bind to specific receptors and kill cells via pore formation; although other modes of action have been proposed (2). A small group of Cry toxins known as parasporins (PS) presents activity against some human cancer cell lines and their application in anti-cancer therapy was suggested (3). Classified into six families PS1-6 (4), they seem to act via different mechanisms, including pore formation (5) and apoptosis (6). Parasporin3 or Cry41Aa is highly selective against human hepatic (HepG2) and myeloid leukaemia (HL-60) cancer cells, while being structurally similar to some commercially used insecticidal Cry toxins (7). We investigated its mode of action and the results are consistent with Cry41Aa being a pore-forming toxin (PFT). The toxin induced extensive membrane damage, cell swelling, rapid decrease in ATP levels and metabolic activity, but no activation of caspases or oxidative stress (8). However, confirmation of specific toxin binding to the plasma membrane was unsuccessful and despite rapid loss of membrane integrity, the nature of permeabilization has never been closely investigated. Here we demonstrate that Cry41Aa formed stable channels in planar lipid bilayers and induced large whole-cell currents in HepG2 cells. Interestingly, we have noticed an inhibitory effect of EGTA on Cry41Aa activity. EGTA, like EDTA, is a non-specific chelator of metal ions commonly used to test the roles of extracellular cations in the activities of various proteins including Cry toxins. It was shown that EDTA decreased pore formation by Cry1Aa, Cry1Ac and Cry1Ea in isolated insect BBMV and the role of cations in Cry toxin binding and pore formation was suggested (9). Extracellular Ca^{2+} was shown to be indispensable for the activity of PS1 (Cry31Aa1) in mediating apoptosis in HeLa cells (6). Extra– and intracellular increases in Ca^{2+} augmented Cry1C toxicity in *Spodoptera frugiperda* Sf9 cells, possibly via a Ca^{2+}-dependent intracellular pathway (10). Toxicity of *Bt* var. *entomocidus* against *Spodoptera littoralis* was enhanced by Ca^{2+} and Zn^{2+} salts (11). However, osmotic swelling assays using *Manduca sexta* BBMV and Cry1 toxins showed some contradictory results; for example, Ca^{2+} increased the rate of pore formation by Cry1Ac, but reduced pore formation by Cry1Ca (12). Moreover, there are reports of synergistic effects of EDTA and Cry toxin-containing Dipel in resistant *Plutella xylostella* larvae (13). Despite a vast amount of literature on the subject, few researchers have addressed the problem of non-target cation binding and tend to focus primarily on a single metal-chelator complex. In this study, the chelator effect is investigated on the activity of Cry41Aa in HepG2 cells, taking into consideration the fact that EGTA forms complexes with a broad number of metal cations, existing both in free- and protein-bound forms.

2. Materials and methods

2.1. Toxin harvesting and purification

Recombinant *Bt* strains were grown for 3 days at 30°C on Luria-Bertani plates with 5 µg/ml chloramphenicol. Cells containing crystals were sonicated in water, washed twice in 0.3 M NaCl, and the pellets were re-suspended in water. The protoxin-spore mixture was solubilized at 37°C for 1 h in 50 mM Na_2CO_3 buffer, pH

10.5 and containing 5 mM DTT. The supernatant was incubated with trypsin (Sigma, UK) for 1h at 37°C in a ratio of 1 mg enzyme per 1 mg protoxin. After activation a protease inhibitor (Roche complete mini EDTA-free, Sigma) was added and the toxin was purified on a 15 ml Sephacryl S-200 High Resolution (Amersham Bioscience) gel filtration column. Fractions were eluted in 25 mM Tris/150 mM NaCl (pH 7.4) and protein concentration was determined by a Bradford assay (Protein Assay Kit, Bio-Rad, UK) using BSA as the standard.

2.2. Cell culture

The HepG2 cell line was purchased from the European Collection of Cell Cultures (ECCAC, Salisbury, UK). Cells were maintained in Dulbecco's modified Eagle's medium (DMEM), high glucose, supplemented with 10% fetal calf serum (FCS), 100 U/mL penicillin, 100 µg/mL streptomycin, 292 µg/mL L-glutamine (referred here as complete DMEM) in 75cm^2 flasks at 37°C in a humidified 5% CO_2 incubator. When the cells reached 70-80% confluency, they were split using 0.05% trypsin-EDTA.

2.3. Cell assays

Unless specified otherwise, 90 µl of cell suspension containing approximately 22,500 HepG2 cells were dispensed in triplicate into a 96-well plate in complete DMEM and 20 h later each well received appropriate treatment. Data are mean values ± S.E.M. of triplicate wells, performed in duplicate experiments. Cell viability was assessed using the CellTiter-Blue assay (Promega, UK) as an endpoint method with a 2-hour incubation with the reagent. Membrane integrity was determined with the CellTox Green cytotoxicity assay (Promega, UK) using 'Express, No-Step Addition at Seeding Method' according to the manufacturer's instructions.

2.4. Experiments with chelators

EDTA and $CaCl_2$ were purchased from AnalaR BDH (Poole, Dorset, UK); $MgCl_2$, Dulbecco's phosphate-buffered saline (DPBS) and cell culture media from ThermoFisher Scientific (UK); EGTA, BAPTA, DTPA from Trocis Bioscience (Abingdon, UK). Other reagents were purchased from Sigma Aldrich (UK). EGTA and EDTA were prepared as a 55 mM stock solution in distilled water (pH adjusted to 8), later diluted in culture medium accordingly. BAPTA and DTPA were prepared according to the manufacturer's guidelines. Mock cells were treated with the equal amount of distilled water only. Initially, cells were pre-treated with 5 mM EGTA 30 min prior to toxin treatment. Later, in light of further results, the dose and time were reduced to 2 mM and 10 min. Periods of cell culture in DPBS without calcium and magnesium, Advanced DMEM (medium allowing cell growth with reduced FCS supplementation) and Ca^{2+}-free DMEM (high glucose, no calcium) were kept to a minimum. Experiments that involved Ca^{2+}-free medium were carried out straight after cell seeding, as lack of extracellular Ca^{2+} led to a detrimental fall in viability after 20 h. For statistical comparison of treatments in salt supplementation experiments, Post-Hoc analysis applying a Bonferroni adjustment was carried out using IBM SPSS Statistics for Windows, version 22.0. (IBM Corp, Armonk, NY, USA). Dose-response curves were generated using nonlinear regression analysis and the equation 'Dose-response – Stimulation, [Agonist] vs. response - Variable slope' in GraphPad Prism version 8.1.0 (GraphPad Software, La Jolla, CA, USA, www.graphpad.com). Calculations of bound and free Ca^{2+}, Mg^{2+} and EGTA were performed using the Ca/Mg/ATP/EGTA calculator version 1, available online: maxchelator.stanford.edu/.

2.5. Western blot analysis

HepG2 cells were seeded at the density of 25 x 10^4 cells/ml in 6-well plates in complete DMEM. After ~70% confluency was achieved, cells were pre-treated with 2 mM EGTA or water for 10 min. Next, sodium arsenite (0.5 mM), Cry41Aa (15 µg/ml) or buffer were added. 15 minutes after toxin treatment, cells were washed twice with DPBS at 4°C, gently scraped, spun at low speed (200 x *g*) and the pellet was lysed at 4°C for 20 min in Tergitol-type NP-40 buffer (150 mM NaCl, 1% NP-40, 50 mM tris, pH 8.0, 2 mM $NaVO_4$, 1 µM microcystin, 1 mM EDTA, 1 mM EGTA with Roche complete mini EDTA-free protease inhibitors). Precleared lysates (20 min at 16,873 x *g*) were subjected to SDS-PAGE and western blot analysis. Proteins were transferred to a nitrocellulose membrane (Bio-Rad) using a Bio-Rad Trans-Blot Semi-Dry Transfer Cell system (100 mA for 60 min). Probing was done overnight at 4°C in blocking solution containing 3% BSA and primary antibody against phospho-p38 (ThermoFisher Scientific, MA5 15182, 1:1000) or CD59 (Abcam, ab126777, 1:50000). The next day membranes were incubated with secondary HRP-conjugated antibody (Abcam, ab97051) and blots developed on X-ray film (FUJI medical X-ray film).

2.6. Whole-cell patch-clamp electrophysiology experiments

HepG2 cells were seeded at 5 x 10^4 cells/ml on 24 mm circular glass coverslips 24 – 48 h before experiments. Cells were washed three times with the bath solution (140 mM NaCl, 5 mM KCl, 1.1 mM $MgCl_2$, 1.1 mM $CaCl_2$, 10 mM HEPES, pH 7.4) and mounted inside a coverslip holder fitted to the microscope stage (IMT-2, Olympus). 1 ml of the bath solution was added. Soda lime pipettes (Kimble Chase) were filled with the pipette solution (140 mM KCl, 1.1 mM $MgCl_2$, 0.1 mM EGTA, 10 mM HEPES, pH 7.4) and had a resistance of around 4 MΩ. The resistance of the seals was in the range of 2-10 GΩ. A −20 mV holding potential and trains of 17 command voltage steps (1-s duration, ranging from −20 to 140 mV, in increments of 10 mV) were applied before and 20 min after the addition of Cry41Aa (12 µg/ml) to the bath in the presence or absence of 2 mM EGTA (added 10 min before the toxin). The command voltages were generated by, and the whole-cell currents were recorded and processed with Axon Digidata 1550 converter (Molecular Devices) and Axopatch – 1D patch-clamp amplifier (Molecular Devices). Currents were filtered at 10 kHz and sampled at 50 kHz. Data collection and analysis were conducted using the pCLAMP 10.6 software (Molecular Devices). Error bars indicate the standard error of the mean. The current – voltage (I/V) curves show the mean currents from three representative experiments on three different patched cells. Conductance levels were calculated from the slope of linear regression line of each I/V curve at 20 min. Experiments were performed at room temperature.

2.7. Planar lipid bilayer experiments

Planar lipid bilayer experiments were performed using the methods described previously (14). A lipid mixture of POPE:POPC:cholesterol (Avanti Polar Lipids, Alabaster, USA) was prepared in a ratio of 7:2:1 (w/w/w). Lipids were dried with N_2 and then dissolved in n-decane at 20 mg/ml. 1 ml of KCl buffer (150 mM KCl, 1 mM $CaCl_2$, 10 mM HEPES, pH 7.5) was added to cis and trans – custom made disposable chambers, equipped with magnetic stirrers. A lipid membrane was painted in a 250 µm diameter hole present at the junction of both chambers with the lipid mixture using a blunt end glass pipette. Chambers were connected to Ag/AgCl electrodes through conducting agar bridges (2 M KCl, 1 mM EGTA and 2% agar) and placed inside a small Faraday enclosure. Voltage was applied to the cis chamber (trans chamber was grounded). Membrane activity

was recorded for 30 min with holding voltages ranging from -150 to +150 mV to ensure no contamination. Capacitance of the membrane was 180 - 200 pF. Cry41Aa was added to the cis chamber at 8 µg/ml and current was recorded at different voltages. All experiments were performed three times, at room temperature. Currents were acquired using Axopatch-1D patch-clamp amplifier (Molecular Devices, Sunnyvale, USA). Currents were filtered at 5 kHz and digitized at 50 kHz with Axon Digidata 1440A (Molecular Devices). Recordings were analysed using pCLAMP 10.5 (Molecular Devices). To measure the conductance, 20-25 current jumps were recorded for each voltage, grouped and averaged. I/V curves were plotted from the data points fitted by linear regression. Mean conductance was read from the slope of each I/V curve regression line. At the end of each experiment, concentration of KCl in the cis chamber was increased to 450 mM, using 3 M KCl, 1 mM $CaCl_2$, 10 mM HEPES, pH 7.5, to measure reversal potential. PK+/PCl- permeability ratios were calculated from the reversal potential using the Goldman-Hodgkin-Katz equation (15).

3. Results

3.1. Effects of chelation on cells and Cry41Aa toxicity

EGTA is thought to be membrane impermeant and not metabolised by living organisms. Ca^{2+}, one of the most abundant divalent metal ions present in extracellular fluid and in DMEM cell culture formulation (Table 1), plays a crucial role in cell physiology (16). It has been shown that removal of extracellular Ca^{2+} reversibly increases permeability of tight junctions, leading to cell contraction and reduction of cell-to-cell adhesion (17). Mouse myoblast C2C12 cells treated with 1.75 mM EGTA for 24 hours showed significant alteration in morphology resulting from changes in number and distribution of stress fibres and microtubules (18). 24-hour HepG2 cell exposure to 2 mM EGTA resulted in ~20% reduction of viability (data not shown). For this reason, all chelator experiments were carried out over a period of up to 6 hours, a time during which no loss of viability or change in cell morphology were noticed (data not shown). HepG2 cells were preincubated with either EGTA or EDTA, followed by toxin administration and viability examination (Fig. 1A). Both EDTA and EGTA significantly reduced the cytotoxicity of Cry41Aa. Cell swelling, a general feature of Cry toxin action (19), was not observed in the chelators' presence. EGTA also prevented phosphorylation of p38 MAP kinase in Cry41Aa-treated cells (Fig. 1B). This signalling pathway, commonly triggered by pore formation (20), was induced by Cry41Aa in the chelator's absence at 15 min after toxin exposure. The signal matched that of sodium arsenite, a potent p38 inducer.

3.2. Analysis of possible indirect effects of EGTA

Extensive measures were taken to ensure that EGTA action resulted from metal ion chelation and no other indirect effect. To test if EGTA was causing the toxin to degrade or precipitate, Cry41Aa was incubated with EGTA (2 or 5 mM) at 37ºC or room temperature, followed by SDS – PAGE. The size and quantity of toxin in the soluble fraction was unaffected by incubation with the chelator under different conditions (data not shown). To test the possibility that the toxin interacted with EGTA and that this affected its toxicity, Cry41Aa was incubated with EGTA, dialysed and tested on cells. Its toxicity was fully retained after dialysis (data not shown). A shift towards more acidic pH was observed in culture medium (from 7.4 to 6.8) upon cell supplementation

with 2 mM EGTA, most likely due to protons being displaced by metal cations in the chelation reaction (21). We therefore investigated the toxicity of Cry41Aa in complete DMEM at lower pH values in the absence of EGTA. Toxin activity was unaffected at pH 6.84 (data not shown).

3.3. Investigation of cations involved in toxicity

Next, cells were additionally supplemented with $CaCl_2$ or $MgCl_2$ to see if toxicity could be restored despite the chelator's presence. Ca^{2+}, but not Mg^{2+}, reinstated cytotoxicity of Cry41Aa in EGTA and EDTA pre-treated cells (Fig. 2). The Ca^{2+} salt reversed the chelator effect whether it was added 30 min before or after the toxin (data not shown). To confirm these results and further investigate any difference between Ca^{2+} and other cations, other chelators were tested at concentrations between 0 and 5 mM (Fig. 3). BAPTA is a derivative of EGTA, designed to be more selective for Ca^{2+} over Mg^{2+} than EGTA; however, it forms lower affinity Ca^{2+}-chelates than EGTA (6.71 versus 7.18 at pH 7.4 (22)). DTPA is a membrane impermeable chelator often used in Zn^{2+} depletion studies. Only Zn^{2+} and, to a lesser extent, Cu^{2+}, but not Ca^{2+} or Mg^{2+}, were able to counteract the cytotoxic effect of DTPA in breast cancer cell lines after 48-hour exposure (23); however, DTPA has the capacity to bind other ions (24). Histidine is a ligand of a few metallic ions including Cu^{2+}, Ni^{2+} and Zn^{2+} (25) but has negligible affinity for Ca^{2+}. For this reason, it has been used alongside EGTA to test the involvement of Ca^{2+} in permeability of lymphocyte membranes (26, 27). In Fig. 3, BAPTA showed comparable results to those with EGTA, with the latter being slightly more efficient at cell protection against Cry41Aa. A higher concentration of DTPA was required to achieve this effect, while histidine had no significant impact, even at higher (up to 10 mM) concentrations (data not shown).

These findings, pointing to a pivotal role of extracellular Ca^{2+} in Cry41Aa toxicity, were challenged in the next experiment conducted in Ca^{2+}-free medium. Titration of EGTA was performed in Ca^{2+}-free DMEM with and without FCS, as well as in complete DMEM (Fig. 4). Cells in DMEM devoid of extracellular Ca^{2+} resisted Cry41Aa at much lower EGTA concentration, compared to complete DMEM. When Ca^{2+}-free DMEM was lacking FCS, which accounts for an additional source of trace metal cations, cells resisted Cry41Aa at even lower chelator dose. More importantly, in the absence of EGTA, toxin retained its activity in Ca^{2+}-free DMEM without FCS, suggesting that EGTA bound other extracellular metal ions or ions (including Ca^{2+}) present in cellular membranes. Chelating properties of EGTA can be calculated for Ca^{2+} and Mg^{2+} at any given pH with the Maxchelator program (http://maxchelator.stanford.edu). In a buffer containing 1.8 mM Ca^{2+} and 0.8 mM Mg^{2+} (levels in DMEM, Table 1) and 2 mM EGTA, 90.8% of the chelator is predicted to be bound at pH 7.4 (37ºC, 0.165 N ionic strength), leaving a portion available to other reactions. The role of other metal ions was examined in their ability to counteract the EGTA effect. Fig. 5 shows that Ca^{2+}, Mn^{2+} and Zn^{2+} supplementation most strongly reinstated Cry41Aa toxicity. Considering that Ca^{2+} counteracted the EGTA effect, we investigated whether increasing extracellular Ca^{2+} levels would increase Cry41Aa toxicity, like for example in the case of Cry1C in Sf9 cells (10). However, adding extra Ca^{2+} did not increase Cry41Aa toxicity in complete DMEM (data not shown). Next, the effect of Ca^{2+} and other metal ions was assessed in Ca^{2+}-free medium and low toxin dose to better visualise viability changes (Fig. 6). In the absence of extracellular Ca^{2+}, low quantities of Mn^{2+} and Zn^{2+} enhanced Cry41Aa toxicity, as did Ca^{2+}. When similar experiments were conducted in the presence of normal Ca^{2+} concentrations (in complete or Advanced DMEM), addition of low levels of Zn^{2+} or Mn^{2+}, but not

Ca^{2+}, also increased Cry41Aa toxicity (data not shown). These findings suggest that cations other than Ca^{2+} can also positively affect toxicity.

We next investigated what would happen to Cry41Aa toxicity in a basic buffer devoid of most metal cations, looking at toxin activity in DPBS in the presence of different BAPTA concentrations (Fig. 7). Much less BAPTA was required to abolish Cry41Aa toxicity in DPBS compared to Advanced DMEM. Also, in the absence of the chelator, like previously observed in Ca^{2+}-free DMEM, the toxin was still able to cause swelling and to decrease cell viability, which suggests that cations bound to the membrane, rather than those in the medium, play a role in Cry41Aa toxicity.

In cation supplementation experiments, addition of extra salts will change the equilibria of existing EGTA chelates. For instance, the addition of a large amount of Zn^{2+} could displace another metal cation from EGTA chelate, making it available to the cells and facilitate toxicity. Also, such high concentrations of trace metal ions like 2 mM Zn^{2+} or Cu^{2+} do not occur in physiological media and have adverse physiological effects on cells (28, 29). A method was developed to avoid the problem of the unknown stoichiometry of each metal ion after supplementation in the presence of EGTA. An experiment was performed where culture medium after EGTA pre-treatment was removed before salt and toxin addition in DPBS (Fig. 8), following the observation that replacing culture medium with DPBS after EGTA pre-treatment still rendered cells resistant to toxin (Fig. 8, first bar). The high viability observed in Cry41Aa-treated cells in DPBS after EGTA removal suggests that, together with removed medium, all the metal cations needed for Cry41Aa toxicity have also been extracted from membranes due to EGTA chelation. Results show that trace levels of Zn^{2+} or Mn^{2+} alone could distinctly reinstate Cry41Aa toxicity. Elevated levels of Ca^{2+} (1 mM), but less than those present in DMEM formulation, not only restored but significantly enhanced toxicity of Cry41Aa, compared to toxin-treated cells where water instead of EGTA was used for transient treatment.

3.4. Investigation of EGTA effect

EGTA was the most efficient chelator tested here at cell protection (Fig. 3), therefore in subsequent experiments we focused on EGTA. To elucidate whether EGTA acts pre- or post-membrane damage, membrane permeability was assessed using the CellTox Green cytotoxic cell assay. In cells exposed to EGTA and Cry41Aa the membrane stayed impermeable to the small cytotoxic marker (<1 kDa) for 6 hours (Fig. 9). For confirmation and more information on the permeabilization process, whole-cell patch-clamp electrophysiological experiments were performed on single HepG2 cells. This sensitive method measures in real time the total ionic currents crossing the cellular membrane as a result of individual ion channel activity in the entire cell probed by the patch-clamp pipette. Cry41Aa induced large currents in HepG2 cells after 20 min exposure to the toxin, compared to the very small currents recorded at time 0, when the toxin treatment was initiated. Such response to the toxin was similar to that of the permeabilizing agent digitonin at 13 µg/ml (data not shown). However, Cry41Aa was not able to induce these large currents in the presence of EGTA after 20 minutes of toxin treatment (Fig 10), or indeed after 5,10,15 or 30 mins of toxin exposure (data not shown). At 20 min, the mean conductance levels were 12.5 and 266.9 nS for cells treated with Cry41Aa in the presence and absence of EGTA, respectively. Also, Cry41Aa had no effect on HeLa or CHOK1 cells (the whole cell currents, in the absence of EGTA, were similar to those observed in HepG2 cells without toxin – data not shown).

Furthermore, another experiment was performed to test for competition between Cry41Aa and EGTA and find out if toxicity could be reversed by late chelator administration (Fig. 11). EGTA was much less able to protect the cells when added more than a few minutes after the toxin, which confirms that it exerts its effect at an early stage in the cytotoxic process.

For more clarification as to whether the chelator impedes toxin binding or the other steps in the mode of action, cell viability was assessed after transient EGTA and Cry41Aa treatment (Fig. 12). A cell washing step after 20-minute incubation ensured that all non-bound toxin molecules and EGTA were removed. As shown in Fig. 12, high viability in cells transiently treated with Cry41Aa and EGTA indicates that the chelator prevented toxin interaction with the membrane within 20 minutes – a time that was sufficient to initiate cytotoxic effects in the chelator's absence. Additional presence of Ca^{2+} throughout the 20-minute period promoted efficient toxicity of Cry41Aa. These results are consistent with a mechanism in which EGTA blocks the toxin from binding to the cell membrane.

Whole-cell patch-clamp experiments indicated that Cry41Aa triggers substantial whole-cell currents either by altering the endogenous channels in HepG2 cell membranes, or by creating channels de novo, or both. To determine the ability of toxin insertion into lipid membranes, channel activity was monitored in planar lipid bilayers. Fig. 14 (left panel), which shows single channel currents in a typical experiment (out of three similar and independent experiments), is the first direct demonstration that Cry41Aa is a pore-forming toxin. Fig. 13 shows the current-voltage relationships derived from unitary channel current measurements in recordings performed at different voltages. Calculated conductances of the most common conducting states or substates of the channels formed by the toxin ranged from 75 to 220 pS and there was no rectification (Fig.13). As shown on the left panel of Fig. 14, one or more channels remained always open at both positive and negative voltages, with only very few short closures, indicative of the channels' opening probability being close to 1. Experiments conducted in 450 mM:150 mM KCl conditions (data not shown) indicated that the channels were slightly cation-selective, with a mean reversal potential from three independent experiments of -10.97 (± 1.00) mV and a PK+/PCl- of 2.48 (± 0.23). Furthermore, EGTA (2 mM) not only did not prevent pore formation by the toxin in planar lipid bilayers, but may even have increased the overall channel currents, as shown on the right panel of Fig. 14, in which the total current at any voltage is larger, suggesting the presence of additional single channels with a similar opening probability close to 1. Further comparative analysis (with and without EGTA) of the channels' activity was made difficult by the fact that there were several channels simultaneously active in the current recordings and that only a few, very short unitary current jumps were observed in each of them. In any case, this data is consistent with EGTA's hypothesised role of binding divalent cations present in biological membranes.

4. Discussion

Bt Cry toxins have been widely used as biopesticides for over 50 years with no harmful effects on humans (30). Parasporins represent a relatively new group of *Bt* toxins that can specifically kill certain human tumour cells in vitro (3). Some parasporins, like Cry41Aa, are closely related in structure to insecticidal Cry toxins; however, at the moment parasporin activity cannot be predicted based on a toxin's sequence. The preferential and narrow

cytocidal activity of Cry41Aa may have potential for anticancer drug design in the future. Our previous research suggested that Cry41Aa kills hepatic liver cancer cells via a pore-forming mechanism (8). In this study, we directly demonstrated its pore-forming nature and investigated the protective role of chelators such as EGTA that renders HepG2 cells resistant to Cry41Aa. Our results indicate that EGTA prevented the toxin's interaction with the cellular membrane, and the subsequent steps of membrane damage and p38 phosphorylation, by chelating metal cations, like Ca^{2+}, Mn^{2+} and Zn^{2+}, present in plasma membrane components and important for Cry41Aa binding.

The chelator action appears to result from metal ion chelation rather than indirect effects, such as interaction with the toxin. Analysis of membrane permeability revealed that the chelator protected cells from membrane damage. This concurs with the fact that EGTA prevented phosphorylation of p38 MAP kinase, a signalling pathway often triggered by pore formation (20). Ratner et al. also demonstrated that EGTA abolished p38 activation in pneumolysin-treated A549 epithelial cells (31). Moreover, a number of investigators demonstrated that non-lytic mutants of some PFTs like *E. coli* hemolysin A or *S. aureus* α-toxin failed to activate p38 (32, 33). EGTA prevented stable interaction between the toxin and the cell membrane, as culturing cells in fresh medium after transient EGTA and toxin treatment resulted in high viability. Further experiments revealed that the later EGTA was administered relative to toxin treatment, the more ineffective it was in cell protection. When a chelator like EGTA is added to a solution, equilibrium is reached relatively quickly within µs to ms, depending on the rate constants of the equilibrium reaction and the ionic strength of the solution. This indicates that the initial few minutes are required for toxin interaction with the membrane. This would be the diffusion time it takes for the toxin to reach and bind membranes but could also include oligomerisation of the toxin. In HepG2 cells exposed to PS2 (Cry46Aa1), membrane associated oligomers were detected after 10 minutes on a ligand blot membrane with the signal reaching its highest intensity after 60 minutes (34). It seems that as soon as EGTA is added, it prevents further toxin action, but it cannot undo the damage already created. This is consistent with the results of a study by Kirouac et al. who showed that EDTA (and, to some extent, EGTA) inhibited the rate of pore formation by Cry1Aa but did not alter the pores that were already formed (9).

Perhaps the most surprising observation in the present study was that EGTA exerted its protective effect by chelating cations bound to plasma membrane components rather than those present in the extracellular medium. This was based on findings that Cry41Aa was active on cells in DPBS or Ca^{2+}-free DMEM without FCS, in the absence of chelators, but minute amounts of EGTA or BAPTA abolished this activity. Both chelators show negligible affinities for K^+ or Na^+, the only two metal ions present in DPBS formulation; therefore, the removal of extracellular cations cannot explain the observed cell protection effect of the chelators. The most plausible explanation is that EGTA's affinity for the cations in question was stronger than the protein-cation affinity in HepG2 cell membranes, pulling them out of their binding partners. Chelator titration curves support the idea of Ca^{2+} being the cation of major importance in Cry41Aa mode of action. BAPTA which forms lower affinity Ca^{2+}-complexes compared to EGTA was somewhat less effective in preventing cell death than EGTA. The ability of high concentrations of DTPA to preserve cell viability was most likely caused by metal chelation other than Zn^{2+}. Whereas 1.2 mM of DTPA was optimal to chelate Zn^{2+} in osteoblastic MC3T3-E1 cells (35), much smaller concentrations (0.1 mM) were successfully used to do so in MCF-7 and MDA-MB468 breast cancer

cells (23). In our experiments, even 2 mM DTPA was not able to fully protect the cells from the toxin's damage. Moreover, histidine, a poor Ca^{2+} chelator, did not inhibit Cry41Aa toxicity.

Significant increase in the whole-cell conductance, to a few hundred nS, was observed in HepG2 cells exposed to Cry41Aa. The most plausible explanation is de novo channel formation rather than activation of endogenous channels, as HepG2 cell channel conductances reported under similar experimental conditions are relatively low. Malhi et al. found that the whole-cell currents from HepG2 cells in the absence of ATP (a K^+ channel inhibitor) were low and ATP-sensitive K^+ channels in these cells required drug stimulation for full channel activation, indicating decreased basal activity of these channels (36). Characterization of single channels in HepG2 cells revealed the presence of calcium- and voltage-dependent channels with conductance values of 18.9 in KCl and 19.8 pS in NaCl solutions in the inside-out configuration, and 22.2 in KCl and 19.7 pS in NaCl solutions in the cell-attached configuration (37). Low amplitude single-channel currents were also recorded in mammalian hepatocytes (38-41). The endogenous HepG2 channel conductances are almost one order of magnitude lower than what was measured in this study using planar lipid bilayers, which suggests that the channel activity underlying the large whole-cell currents observed in the present study most likely correspond to larger conductances from pores made by the toxin itself. However, contribution of endogenous channel activity cannot be completely ruled out. Indeed, it has been demonstrated before that the initial response of Sf9 insect cells to Cry1C exposure involved a calcium influx via voltage-dependent Ca^{2+} channels (42). Here, planar lipid bilayer experiments provided evidence for the formation of stable, slightly cationic channels with multiple conductance levels, suggesting either different substates of a single channel population or a few separate channel populations, or both. For comparison, conductance values for other Cry toxins in planar lipid bilayers were, when determined under symmetrical 150mM KCl conditions: 461 pS for Cry1Ac, 350 pS for Cry1B, 90 pS for Cry1C, 450 pS for Cry1Aa (43), 125 pS or less for Cry5B (44), and 11, 16 and 21 pS for a PS1 homolog – Cry31Aa2 (45). The lack of effect of EGTA on Cry41Aa activity in planar lipid bilayers most likely resulted from the use of a simple experimental channel reconstitution system made of lipid bilayers that are devoid of cellular membrane proteins and thus do not allow for cation binding to the artificial membranes. On the other hand, the EGTA preventive action observed in whole-cell experiments implies that Cry41Aa mode of action in biological membranes of susceptible cells is fully facilitated with the help of specific binding molecules (so-called receptors), whose integrity or function, or both, are associated with metal cations. This is also supported by the resistance of HeLa or CHOK1 cells to the toxin at the electrophysiological level, which most likely lack these receptors.

Table 1 presents formation constants for some of metal-EGTA complexes. However, EGTA-metal equilibria are calculated with only one type of cation present and in a situation when EGTA is fully dissociated at alkaline pH (at physiological pH complexes will be less stable). Since EGTA forms complexes with many metallic cations, it is difficult to predict the levels of the un-chelated free metal ions available to cells after EGTA treatment in culture medium. What is known is that both the abundance of metal ions (if they are major constituents in DMEM like Ca^{2+} or Mg^{2+} or minor like Zn^{2+} or Mn^{2+}) and their ability to form stable complexes with the chelator at experimental pH, will highly influence the actual equilibria (21). Considering that the biological levels of Zn^{2+} and Mn^{2+} are in the µM and nM range respectively and that EGTA-metal stability constants are higher for Mn^{2+}, Zn^{2+}, etc. than for Ca^{2+} (46), the addition of large quantities of Zn^{2+} or Mn^{2+} in some of our

experiments most likely created variations in the equilibrium concentrations of all the strongly chelated as well as un-chelated ions releasing other ions that formed less stable complexes with EGTA. For example, added Zn^{2+} could displace Ca^{2+}, which when released could facilitate Cry41Aa action. However, when EGTA was present in the cell medium throughout the experiments, results were comparable to those of experiments where ion supplementation was done in the chelator's absence or after its removal, as summarized in the cartoon shown in Fig. 15. Our findings highlight the role of Mn^{2+}, Zn^{2+} and Ca^{2+} in Cry41Aa toxicity.

Ions play important roles in cellular metabolism and extracellular processes, yet there is no unified view on the role of divalent cations in Cry toxin mode of action. PS1 (Cry31Aa1) seems to use changes in the cytosolic Ca^{2+} concentration as a messenger system. This toxin induced influx of extracellular Ca^{2+} and apoptosis, by activating trimeric G-protein signalling, as suramin, which inhibits this pathway, suppressed both the Ca^{2+} influx and cytotoxicity of PS1-treated HeLa cells (6). Fortier et al. also highlighted the importance of divalent cations, ionic strength and pH in the Cry toxin mechanism of action (12). These authors postulated that binding and pore formation could be influenced by electrostatic interactions between the toxin molecules and the membrane. Experiments using membrane potential measurements and osmotic swelling assays with insect BBMV showed that at higher pH values, both ionic strength and divalent cations screen negative charge at both the toxin and membrane surfaces increasing their interaction (12). Finally, Kirouac et al. demonstrated that EDTA inhibited pore formation by Cry1Aa, Cry1Ac, and Cry1Ea in isolated BBMV, a system devoid of cellular content and metabolism, suggesting the role of metal ions in processes other than signalling pathways (9). In contrast to PS1, extracellular cations are not mandatory for Cry41Aa activity. Our results indicate that EGTA acted at an early stage, preventing an effective toxin interaction with the membrane by means of chelating membrane bound ions. A large number of proteins are found that coordinate factors - often metal ions - to facilitate specific functions and help stabilize protein structures (47). Changes in the conformation or functionality of a membrane receptor(s) could account for the results presented in this study and was proposed before to explain the EDTA effect on Cry1 toxins (9). Upon the addition of EDTA, a large conformational transition occurs in a cadherin structure, from a rod-like to globular shape (48). It has been further shown by Candas et al. that Ca^{2+} removal mediates cleavage of the ectodomain of cadherin BT-R1 – a target receptor for Cry1A toxin - leading to its destabilisation and proteolytic cleavage (49). Ca^{2+}, Zn^{2+} and Mn^{2+} most prominently reinstated Cry41Aa toxicity and, crucially, after transient EGTA treatment. Our observations may suggest the presence of multiple receptors. Interestingly Zn^{2+}-dependent metalloproteases (aminopeptidase N APN), Zn^{2+}-binding proteins (alkaline phosphatase ALP) and Ca^{2+}-stabilised proteins (cadherin-like proteins) have previously been identified as functional Cry toxin receptors in insects (50). The possibility that metal cations facilitate Cry41Aa toxicity in a cooperative fashion appears quite plausible in light of the present work. Cry41Aa may require more than one receptor to be active, each coordinating a different metal. Such a multiple receptor requirement has been proposed in the sequential binding model in which both APN and cadherin receptors have been suggested for Cry1Ab toxicity towards *M. sexta* (51). Another possibility is that the identified metal ions show functional redundancy in the main receptor (following EGTA facilitated metal release, a different metal can be selected for to maintain protein's structure and/or function), as proteins often adopt flexible metal binding sites, allowing non-specific interactions with many divalent metal cations depending on their bioavailability (52).

5. Conflict of interest

The authors declare no conflict of interest.

6. Acknowledgements

BD would like to thank the Biotechnology and Biological Sciences Research Council and the University of Sussex for funding her PhD studentship. The electrophysiology work was supported by the Research Opportunity Fund funded by the University of Sussex. MJW is funded by grants from the Medical Research Council (MR/K01952X/1) and Bloodwise (12035 and 15024). JLS was supported by a grant from the Natural Sciences and Engineering Council of Canada (CRDPJ 44052-12) and EF by a Université de Montréal graduate student scholarship.

7. References

1. Adang MJ, Crickmore N, Jurat-Fuentes JL. Chapter two - Diversity of *Bacillus thuringiensis* crystal toxins and mechanism of action. In: Tarlochan SD, Sarjeet SG, editors. Advances in Insect Physiology: Academic Press; 2014. pp. 39-87.
2. Vachon V, Laprade R, Schwartz JL. Current models of the mode of action of *Bacillus thuringiensis* insecticidal crystal proteins: a critical review. J Invertebr Pathol. 2012;111.
3. Ohba M, Mizuki E, Uemori A. Parasporin, a new anticancer protein group from *Bacillus thuringiensis*. Anticancer Research. 2009;29:427 - 34.
4. Okumura S, Ohba M, Mizuki E, Crickmore N, Côté J-C, Nagamatsu Y, et al. Parasporin classification and nomenclature. http://parasporinfitcpreffukuokajp/ 2013 (Accessed 4th Feb 2013).
5. Kitada S, Abe Y, Shimada H, Kusaka Y, Matsuo Y, Katayama H, et al. Cytocidal actions of parasporin-2, an anti-tumor crystal toxin from *Bacillus thuringiensis*. Journal of Biological Chemistry. 2006 Sept 8;281(36):26350-60.
6. Katayama H, Kusaka Y, Yokota H, Akao T, Kojima M, Nakamura O, et al. Parasporin-1, a novel cytotoxic protein from *Bacillus thuringiensis*, induces Ca^{2+} influx and a sustained elevation of the cytoplasmic Ca^{2+} concentration in toxin-sensitive cells. Journal of Biological Chemistry. 2007 Mar 9;282(10):7742-52.
7. Yamashita S, Katayama H, Saitoh H, Akao T, Park YS, Mizuki E, et al. Typical three-domain cry proteins of *Bacillus thuringiensis* strain A1462 exhibit cytocidal activity on limited human cancer cells. Journal of Biochemistry. 2005 Dec;138(6):663-72.
8. Krishnan V, Domanska B, Elhigazi A, Afolabi F, West MJ, Crickmore N. The human cancer cell active toxin Cry41Aa from *Bacillus thuringiensis* acts like its insecticidal counterparts. Biochem J. 2017 Mar 24.

9. Kirouac M, Vachon V, Quievy D, Schwartz J-L, Laprade R. Protease inhibitors fail to prevent pore formation by the activated *Bacillus thuringiensis* toxin Cry1Aa in insect brush border membrane vesicles. Applied and environmental microbiology. 2006;72(1):506-15.
10. Monette R, Potvin L, Baines D, Laprade R, Schwartz JL. Interaction between calcium ions and *Bacillus thuringiensis* toxin activity against Sf9 cells (*Spodoptera frugiperda*, Lepidoptera). Applied and environmental microbiology. 1997 Feb 1;63(2):440-7.
11. Salama HS, Foda MS, Sharaby A. Potential of some chemicals to increase the effectiveness of *Bacillus thuringiensis Berl*. against *Spodoptera littoralis* (*Boisd*.). Zeitschrift für Angewandte Entomologie. 1985;100(1-5):425-33.
12. Fortier M, Vachon V, Kirouac M, Schwartz JL, Laprade R. Differential effects of ionic strength, divalent cations and pH on the pore-forming activity of *Bacillus thuringiensis* insecticidal toxins. J Membr Biol. 2005 Nov;208(1):77-87.
13. Liu Y-B, Tabashnik BE. Synergism of *Bacillus thuringiensis* by ethylenediamine tetraacetate in susceptible and resistant larvae of diamondback moth (Lepidoptera: Plutellidae). Journal of Economic Entomology. 1997;90(2):287-92.
14. Fortea E, Lemieux V, Potvin L, Chikwana V, Griffin S, Hey T, et al. Cry6Aa1, a *Bacillus thuringiensis* nematocidal and insecticidal toxin, forms pores in planar lipid bilayers at extremely low concentrations and without the need of proteolytic processing. J Biol Chem. 2017 Aug;292(32):13122-32.
15. Hille B. Ion channels of excitable membranes. Third edition. ed: Sunderland, Mass. : Sinauer; 2001.
16. Brini M, Ottolini D, Cali T, Carafoli E. Calcium in Health and Disease. In: Sigel A, Sigel H, Sigel RKO, editors. Interrelations between Essential Metal Ions and Human Diseases. Dordrecht: Springer Netherlands. 2013. pp 81-137.
17. Pitelka DR, Taggart BN, Hamamoto ST. Effects of extracellular calcium depletion on membrane topography and occluding junctions of mammary epithelial cells in culture. The Journal of Cell Biology. 1983 Mar 1;96(3):613-24.
18. Mermelstein CS, Rebello MIL, Amaral LM, Costa ML. Changes in cell shape, cytoskeletal proteins and adhesion sites of cultured cells after extracellular Ca^{2+} chelation. Brazilian Journal of Medical and Biological Research. 2003;36:1111-6.
19. Knowles BH, Ellar DJ. Colloid-osmotic lysis is a general feature of the mechanism of action of *Bacillus thuringiensis* δ-endotoxins with different insect specificity. Biochimica et Biophysica Acta (BBA) - General Subjects. 1987;924(3):509-18.
20. Porta H, Cancino-Rodezno A, Soberón M, Bravo A. Role of MAPK p38 in the cellular responses to pore-forming toxins. Peptides. 2011;32(3):601-6.
21. Spencer CP. The Chemistry of ethylenediamine tetra-acetic acid in sea water. Journal of the Marine Biological Association of the United Kingdom. 1958;37(01):127-44.
22. Bolsover S. A practical guide to the study of calcium in living cells: edited by Richard Nuccitelli, Academic Press. ISBN 0 12 522810 4. Trends in Cell Biology. 1994;4(12):443.
23. Hashemi M, Ghavami S, Eshraghi M, Booy EP, Los M. Cytotoxic effects of intra and extracellular zinc chelation on human breast cancer cells. European Journal of Pharmacology. 2007;557(1):9-19.

24. Byegård J, Skarnemark G, Skålberg M. The stability of some metal EDTA, DTPA and DOTA complexes: Application as tracers in groundwater studies. Journal of Radioanalytical and Nuclear Chemistry. [journal article]. 1999;241(2):281-90.
25. Leberman R, Rabin BR. Metal complexes of histidine. Transactions of the Faraday Society. [10.1039/TF9595501660]. 1959;55(0):1660-70.
26. Quastel MR, Segel GB, Lichtman MA. The effect of calcium chelation on lymphocyte monovalent cation permeability, transport and concentration. J Cell Physiol. 1981 May;107(2):165-70.
27. Segel GB, Simon W, Lichtman AH, Lichtman MA. The activation of lymphocyte plasma membrane (Na,K)-ATPase by EGTA is explained better by zinc than calcium chelation. J Biol Chem. 1981 Jul 10;256(13):6629-32.
28. Plum LM, Rink L, Haase H. The Essential Toxin: Impact of Zinc on Human Health. International Journal of Environmental Research and Public Health. 2010;7;1342-1365.
29. Bulcke F, Dringen R, Scheiber IF. Neurotoxicity of Copper. In: Aschner M, Costa LG (eds.) Neurotoxicity of Metals. Cham: Springer International Publishing. 2017. pp 313-343.
30. Koch MS, Ward JM, Levine SL, Baum JA, Vicini JL, Hammond BG. The food and environmental safety of *Bt* crops. Frontiers in Plant Science. 2015;6:283.
31. Ratner AJ, Hippe KR, Aguilar JL, Bender MH, Nelson AL, Weiser JN. Epithelial cells are sensitive detectors of bacterial pore-forming toxins. Journal of Biological Chemistry. 2006 May 5;281(18):12994-8.
32. Husmann M, Dersch K, Bobkiewicz W, Beckmann E, Veerachato G, Bhakdi S. Differential role of p38 mitogen activated protein kinase for cellular recovery from attack by pore-forming *S. aureus* alpha-toxin or streptolysin O. Biochem Biophys Res Commun. 2006 Jun 16;344(4):1128-34.
33. Kloft N, Busch T, Neukirch C, Weis S, Boukhallouk F, Bobkiewicz W, et al. Pore-forming toxins activate MAPK p38 by causing loss of cellular potassium. Biochemical and Biophysical Research Communications. 2009;385(4):503-6.
34. Abe Y, Shimada H, Kitada S. Raft-targeting and oligomerization of parasporin-2, a *Bacillus thuringiensis* crystal protein with anti-tumour activity. Journal of Biochemistry. 2008;143(2):269-75.
35. Cho Y-E, Lomeda R-AR, Ryu S-H, Lee J-H, Beattie JH, Kwun I-S. Cellular Zn depletion by metal ion chelators (TPEN, DTPA and chelex resin) and its application to osteoblastic MC3T3-E1 cells. Nutrition Research and Practice. 2007 Spring;1(1):29-35.
36. Malhi H, Irani AN, Rajvanshi P, Suadicani SO, Spray DC, McDonald TV, et al. KATP channels regulate mitogenically induced proliferation in primary rat hepatocytes and human liver cell lines: implications for liver growth control and potential therapeutic targeting. Journal of Biological Chemistry. 2000 Aug 25;275(34):26050-7.
37. Chen WH, Yeh TH, Tsai MC, Chen DS, Wang TH. Characterization of Ca(2+)- and voltage-dependent nonselective cation channels in human HepG2 cells. J Formos Med Assoc. 1997 Jul;96(7):503-10.
38. Bear CE. A nonselective cation channel in rat liver cells is activated by membrane stretch. American Journal of Physiology - Cell Physiology. 1990 Mar 01;258(3):C421-C8.
39. Breit S, Kolb H-A, Apfel H, Haberland C, Schmitt M, Häussinger D, et al. Regulation of ion channels in rat hepatocytes. Pflügers Archiv. 1997;435(2):203-10.

40. Koumi S SR, Aramaki T. Characterization of the calcium-activated chloride channel in isolated guinea-pig hepatocytes. The Journal of General Physiology. 1994;104(2):357-73.
41. Capiod T, Ogden DC. The properties of calcium-activated potassium ion channels in guinea-pig isolated hepatocytes. The Journal of Physiology. 1989;409:285-95.
42. Schwartz J-L, Garneau L, Masson L, Brousseau R. Early response of cultured lepidopteran cells to exposure to δ-endotoxin from *Bacillus thuringiensis*: Involvement of calcium and anionic channels. Biochimica et Biophysica Acta (BBA) - Biomembranes. 1991 Jun 18;1065(2):250-60.
43. Schwartz J-L, Lu Y-J, Söhnlein P, Brousseau R, Laprade R, Masson L, et al. Ion channels formed in planar lipid bilayers by *Bacillus thuringiensis* toxins in the presence of *Manduca sexta* midgut receptors. FEBS Letters. 1997;412(2):270-6.
44. Kao C-Y, Los FCO, Huffman DL, Wachi S, Kloft N, Husmann M, et al. Global functional analyses of cellular responses to pore-forming toxins. PLoS Pathog. 2011;7(3):e1001314.
45. Gabriel Narvaez VV, Dong Xu, Jean-Charles Côté, Jean-Louis Schwartz. PS1Aa2 induces ionic channels in lipid bilayer membranes and calcium oscillations in sensitive cells. Paper presented at: 47th Annual Meeting of the Society for Invertebrate Pathology in Mainz, Germany. 2014 Aug 3-7.
46. K. L.Cheng KU, T. lmamura ebs. CRC Handbook of Organic Analytical Reagents. 1982 (CRC Press).
47. Wittung-Stafshede P. Role of Cofactors in Protein Folding. Accounts of Chemical Research. 2002, 35, 201-208.
48. Pokutta S, Herrenknecht K, Kemler R, Engel J. Conformational changes of the recombinant extracellular domain of E-cadherin upon calcium binding. Eur J Biochem. 1994 Aug 1;223(3):1019-26.
49. Candas M, Francis BR, Griko NB, Midboe EG, Bulla LA. Proteolytic cleavage of the developmentally important cadherin BT-R1 in the midgut epithelium of *Manduca sexta*. Biochemistry. 2002 Nov 01;41(46):13717-24.
50. Pigott CR, Ellar DJ. Role of receptors in *Bacillus thuringiensis* crystal toxin activity. Microbiology and Molecular Biology Reviews. 2007 Jun 1;71(2):255-81.
51. Pacheco S, Gómez I, Arenas I, Saab-Rincon G, Rodríguez-Almazán C, Gill SS, et al. Domain II Loop 3 of *Bacillus thuringiensis* Cry1Ab toxin is involved in a "ping pong" binding mechanism with *Manduca sexta* aminopeptidase-N and cadherin receptors. Journal of Biological Chemistry. 2009 Nov 20;284(47):32750-7.
52. Babor M, Greenblatt HM, Edelman M, Sobolev V. Flexibility of metal binding sites in proteins on a database scale. Proteins: Structure, Function, and Bioinformatics. 2005 Feb 22;59, 221-230.

8. Figure and table legend

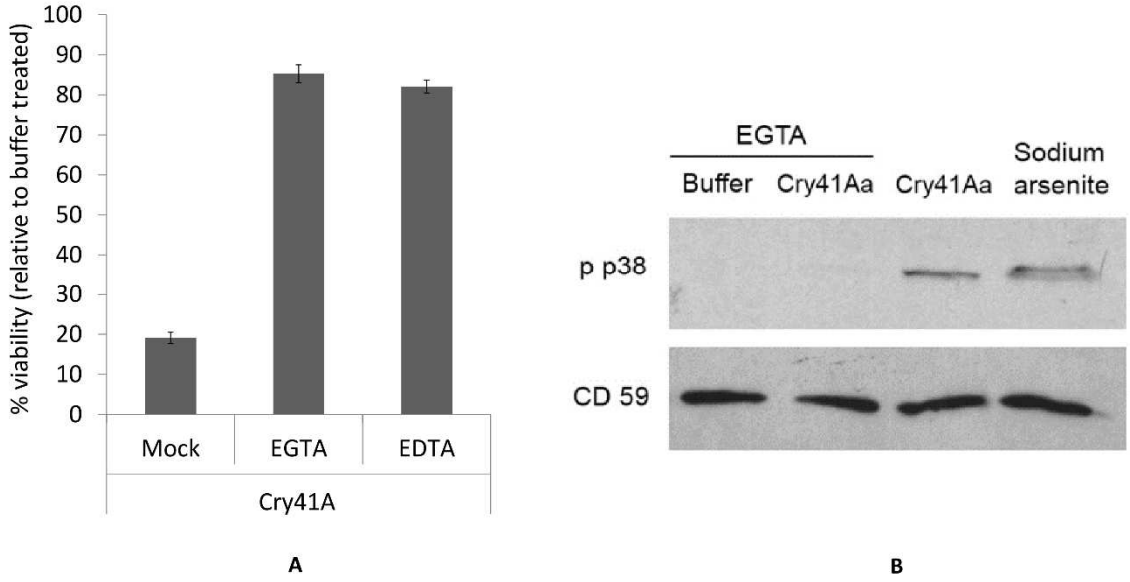

Figure 1 Effect of EGTA on Cry41Aa toxicity in HepG2 cells.

Analysis of viability (A) and p38 phosphorylation (B) was assessed in chelator pre-treated HepG2 cells exposed to Cry41Aa. A) Cells were seeded in complete DMEM. The next day, the cells were preincubated with 5 mM of either EGTA or EDTA or mock for 30 min followed by the addition of Cry41Aa (12 µg/ml). The readings were taken 5 h after toxin addition using the CellTiter-Blue assay. B) HepG2 cells were pre-treated with 2 mM EGTA or water for 10 min. Next, sodium arsenite (0.5 mM), Cry41Aa (15 µg/ml) or buffer were added. Cells were lysed in NP-40 15 min after toxin treatment. 10 µg of proteins were loaded in each lane and after SDS-PAGE proteins were subject to western blot analysis for the presence of phosphorylated p38 (p p38) and CD59 (loading control).

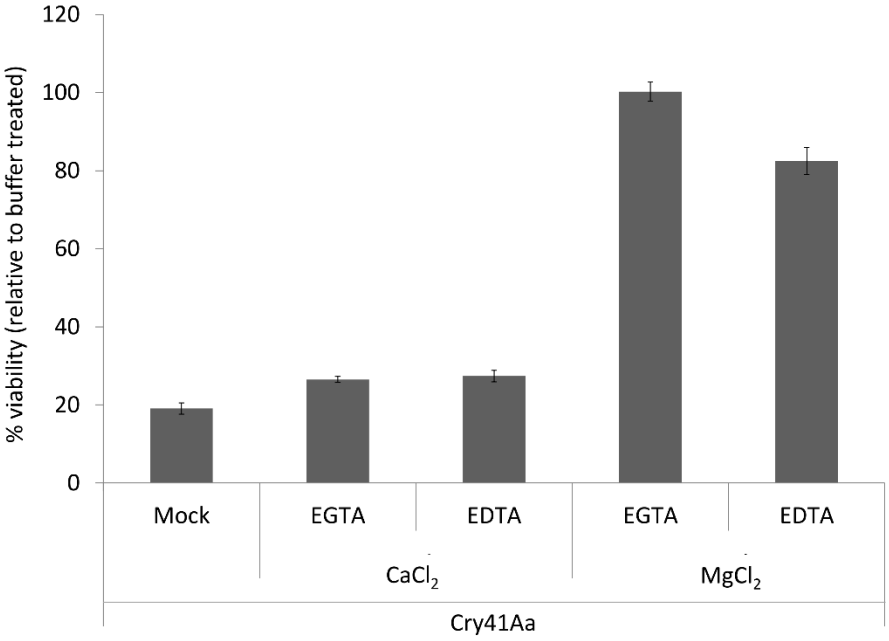

Figure 2 Effect of supplemental Ca^{2+} and Mg^{2+} ions on the chelator induced suppression of Cry41Aa activity.

Cells were seeded in complete DMEM. The next day cells were preincubated with 5mM of either EGTA or EDTA or mock for 30 min followed by the addition of Cry41Aa (12 µg/ml). 5 mM of $CaCl_2$ or $MgCl_2$ was added to the appropriate wells 10 min before the toxin. The readings were taken 5 h after toxin addition using the CellTiter-Blue assay.

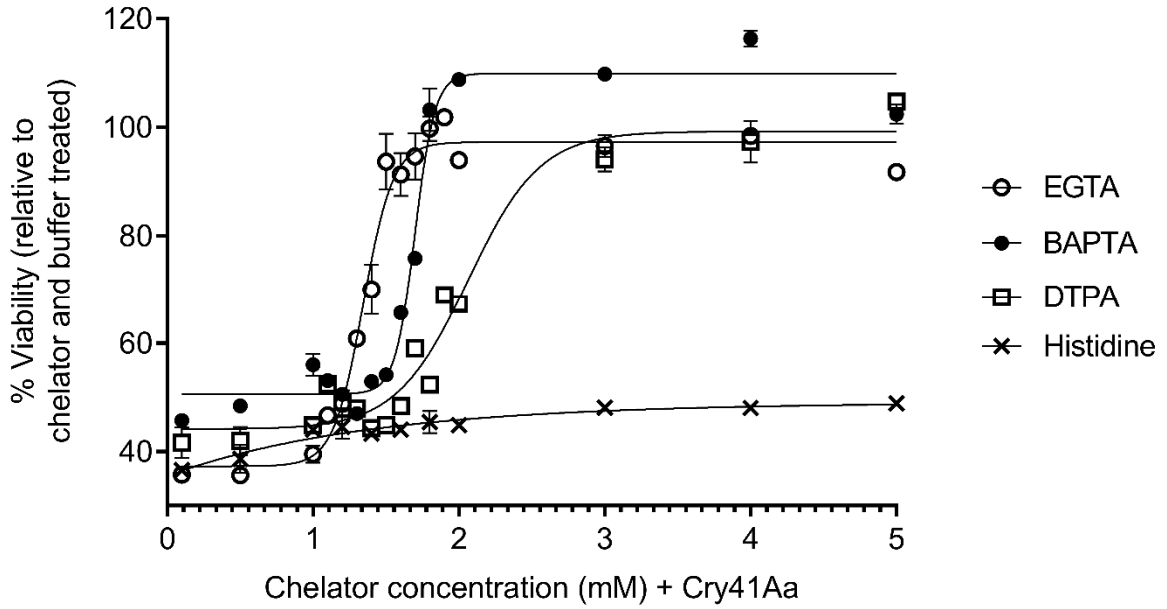

Figure 3 The effect of different metal chelators on Cry41Aa toxicity.

Cells were seeded in Advanced DMEM. The next day, cells were incubated for 30 min with different concentrations of EGTA, BAPTA, DTPA or histidine before Cry41Aa (10 µg/ml) was added. Viability was measured 5 h after toxin addition using the CellTiter-Blue assay.

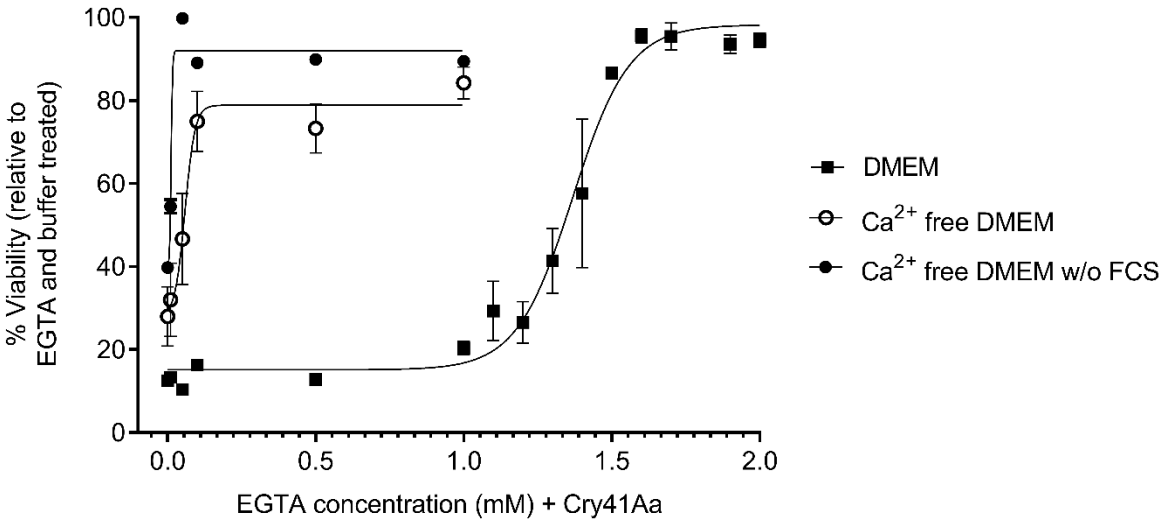

Figure 4 EGTA titration in DMEM with different Ca^{2+} levels and its effect on Cry41Aa activity.

Cells were seeded in complete DMEM and Ca^{2+}-free DMEM with or without FCS. Cells in complete DMEM were seeded 24 h before the experiment and cells in Ca^{2+}-free DMEM on the same day. Cells were treated with different concentrations of EGTA and 30 min later with Cry41Aa (12 µg/ml). CellTiter-Blue cell viability assay was used to measure viability 5 h later.

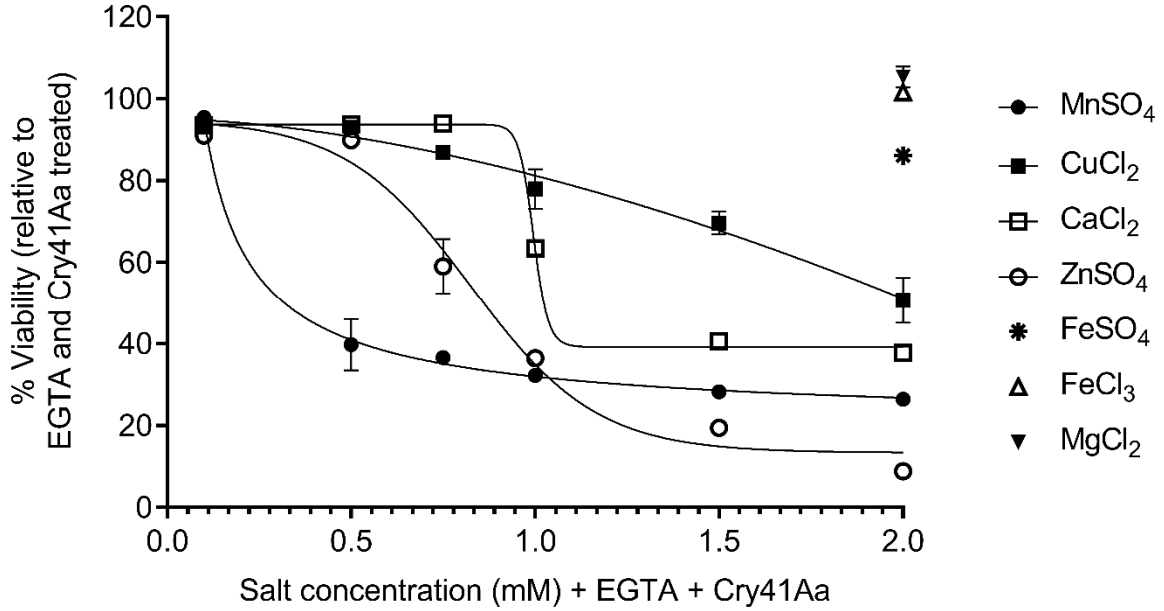

572

573 **Figure 5 Effect of different salts on cells exposed to EGTA and Cry41Aa in Ca^{2+}-free DMEM.**

574 Cells were seeded in Ca^{2+}-free medium followed by treatment with 2 mM EGTA or water. 10 min later different
575 concentrations of salts were added followed by either Cry41Aa (10 µg/ml) or buffer treatment. Viability was measured 5 h
576 later using the CellTiter-Blue assay. Addition of >1 mM of $ZnSO_4$ and $CuCl_2$ to cells resulted in decreased viability (~35%
577 and 15% viability drop in cells treated with 2 mM $CuCl_2$ and $ZnSO_4$ respectively) therefore normalisation was done for the
578 effect of all salts. Normalized data was then plotted as a percentage of the EGTA- and Cry41Aa-treated cells.

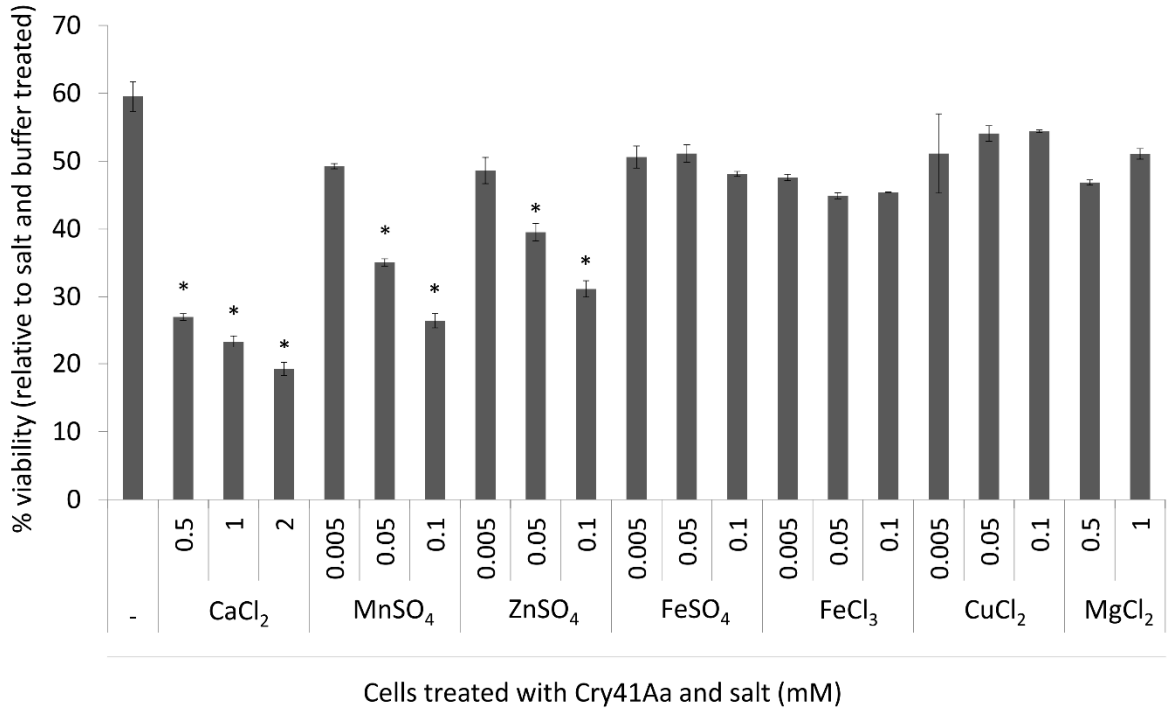

579

580 **Figure 6 The effect of metal salts on residual Cry41Aa toxicity in Ca^{2+}-free DMEM.**

581 Cells were seeded in Ca^{2+}-free DMEM. After 30 min cells were supplemented with various concentrations of metal salts:
582 $CaCl_2$, $MnSO_4$, $ZnSO_4$, $FeSO_4$, $FeCl_3$, $CuCl_2$ or $MgCl_2$, followed by either Cry41Aa (5 µg/ml) or buffer treatment. Viability
583 was measured 5 h after toxin treatment using the CellTiter-Blue assay. Bars with asterisks are significantly different from

control cells exposed to Cry41Aa (5 µg/ml) in Ca^{2+}-free DMEM without supplementation (* p< 0.005, Post-Hoc comparison with Bonferroni correction).

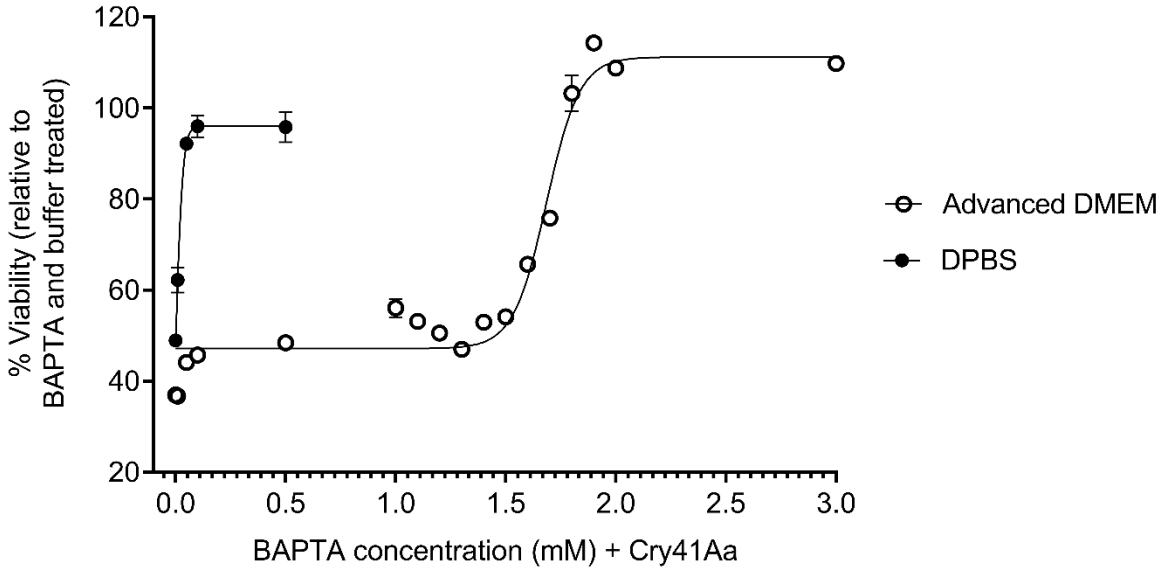

Figure 7 Titration of BAPTA in Advanced DMEM and DPBS and its effect on Cry41Aa activity.

BAPTA in DPBS treatment: cells were seeded in Advanced DMEM. The next day cells were washed once with DPBS and fresh DPBS was placed in the wells. Different concentrations of BAPTA were added and 30 min later Cry41Aa was administered (10 µg/ml). Viability was measured 3 h later using the CellTiter-Blue assay. BAPTA in Advanced DMEM treatment: cells were seeded in Advanced DMEM. The next day cells were incubated with different concentrations of BAPTA. After 30 min Cry41Aa (10 µg/ml) was added and viability was measured 5 h later using CellTiter-Blue assay.

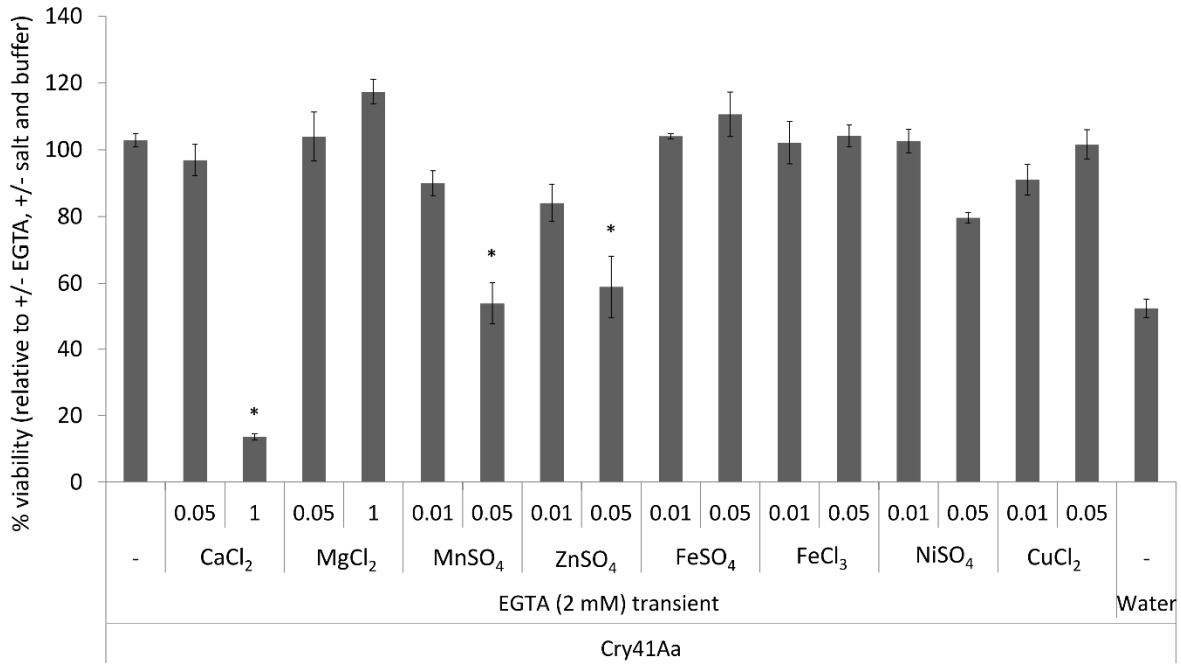

Figure 8 Effect of different salts on Cry41Aa-treated cells in DPBS after EGTA removal.

Cells were seeded in complete DMEM. The next day cells were treated with 2 mM EGTA or water for 10 min. After that the medium was removed from wells and DPBS was added. Five min later different concentrations of salts or water were added, followed by either Cry41Aa (10 µg/ml) or buffer treatment. Viability was measured 4 h later using the CellTiter-Blue assay. Data was plotted as a percentage of the cells treated +/-chelator, +/-salt and with buffer. Bars with asterisks show significant differences from control (cells exposed to Cry41Aa at 10 µg/ml in DPBS without salt supplementation after transient

treatment with 2 mM EGTA - first bar), * p< 0.001, Post-Hoc comparison with Bonferroni correction. Cell incubation with 0.05 mM $CuCl_2$ in DPBS resulted in decreased cell viability (20%) after 4 h, masked here by data normalisation.

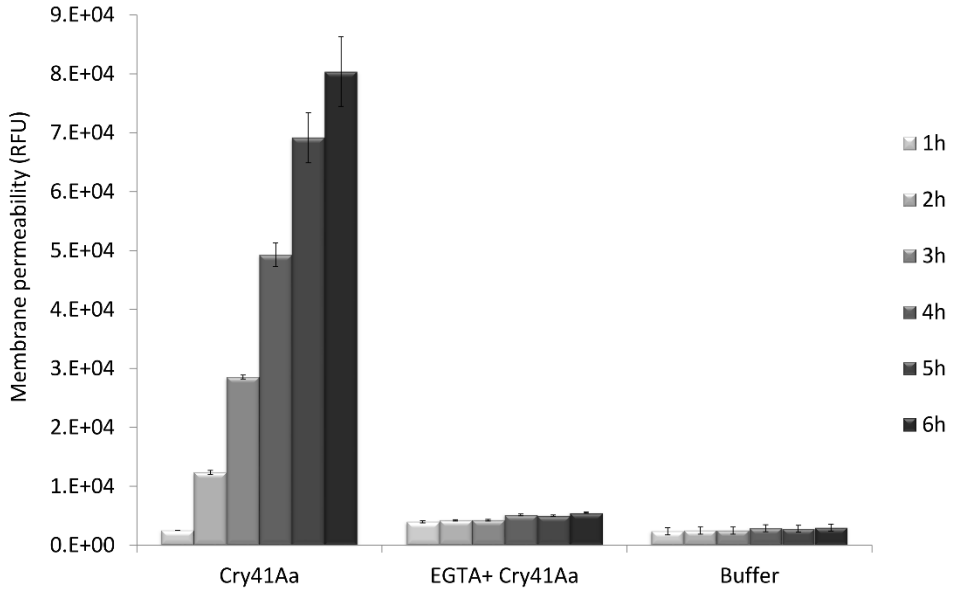

Figure 9 Effect of EGTA on HepG2 cell membrane permeability.

HepG2 cells were seeded in complete DMEM in the presence of CellTox Green dye in a black 96-well plate. The next day, cells were pre-treated with 5 mM EGTA or mock 30 min before treatment with Cry41Aa (12 µg/ml) or buffer. Membrane permeability was measured using the CellTox Green cytotoxicity assay at different times after toxin addition.

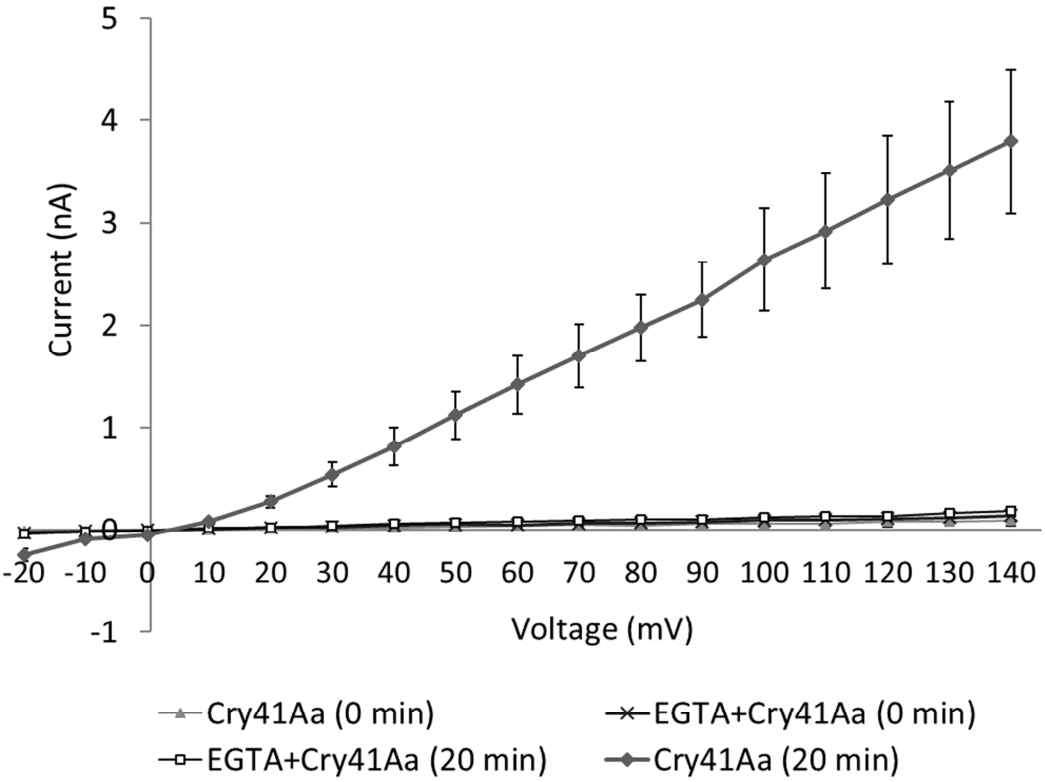

Figure 10 Whole-cell patch-clamp recordings from cells exposed to Cry41Aa in the presence or absence of EGTA.

Whole-cell patch-clamp recordings from a single cell were reported at 0 and 20 min after the addition of Cry41Aa (12 µg/ml) to the bath in the presence or absence of 2 mM EGTA. Currents were induced by a 1 second set of depolarizing

potentials from -20 to 140 mV from a holding potential of -20 mV. The lines show the mean currents from three representative experiments from three different patched cells. Error bars indicate the standard error of the mean.

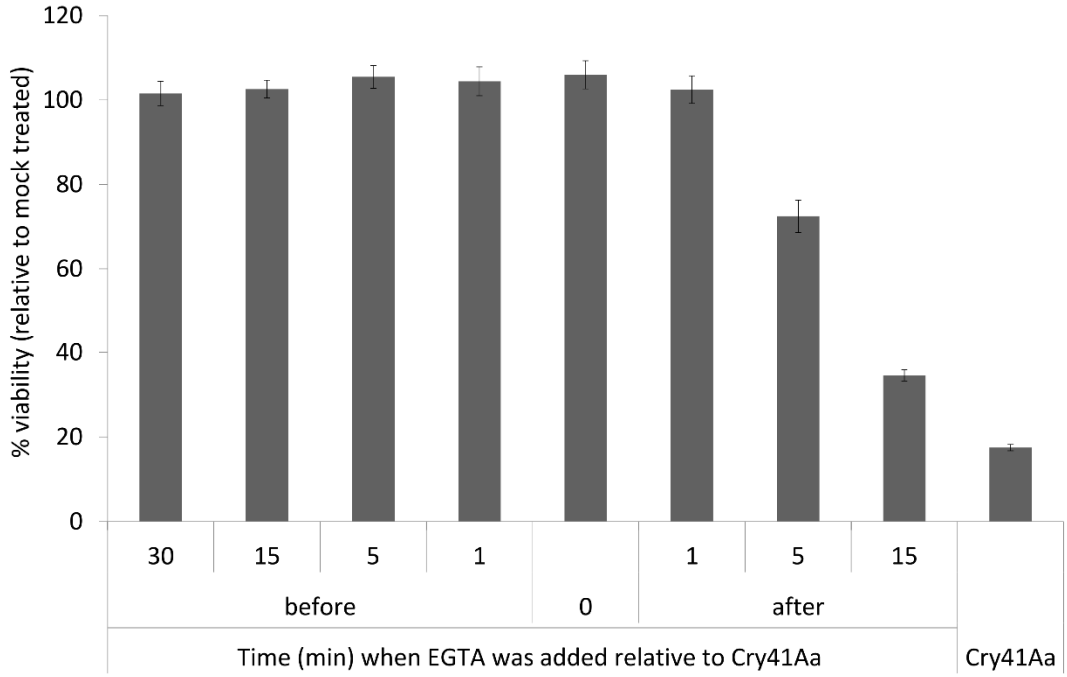

Figure 11 Administration time-dependent effect of EGTA.

Cells were seeded in complete DMEM. The next day cells were treated with 2 mM EGTA at different time points: before, at the same time as, or after Cry41Aa (12 µg/ml). Viability was measured 6h after toxin addition using the CellTiter-Blue assay. Control cells were treated with water and exposed to Cry41Aa (12 µg/ml) for 6 h.

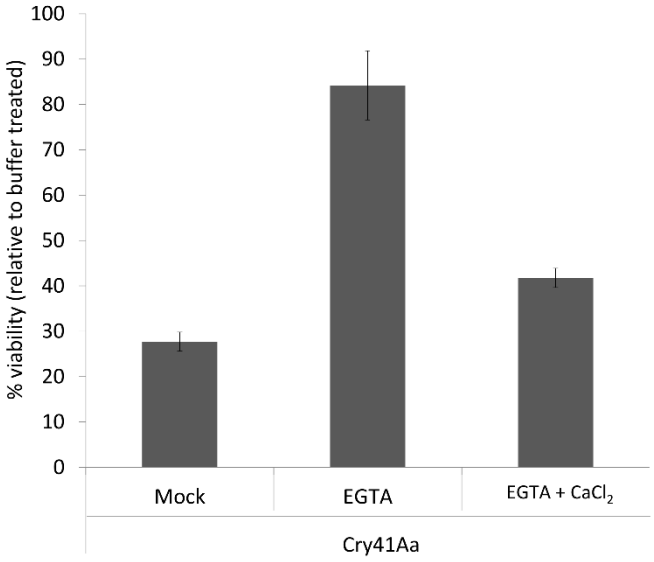

Figure 12 Effect of transient treatment with Cry41Aa and EGTA on cell viability.

Cells were seeded in complete DMEM. The next day cells were preincubated with either 5 mM EGTA or 5 mM EGTA and 5 mM $CaCl_2$ or mock. After 30 min Cry41Aa (12 µg/ml) or buffer was added, and cells were incubated for further 20 min. Then all cells were washed twice with DPBS and re-suspended in complete DMEM. Viability was assessed using the CellTiter-Blue assay 24 h after toxin addition. Results are represented as % viability relative to cells washed after treatment with EGTA and buffer.

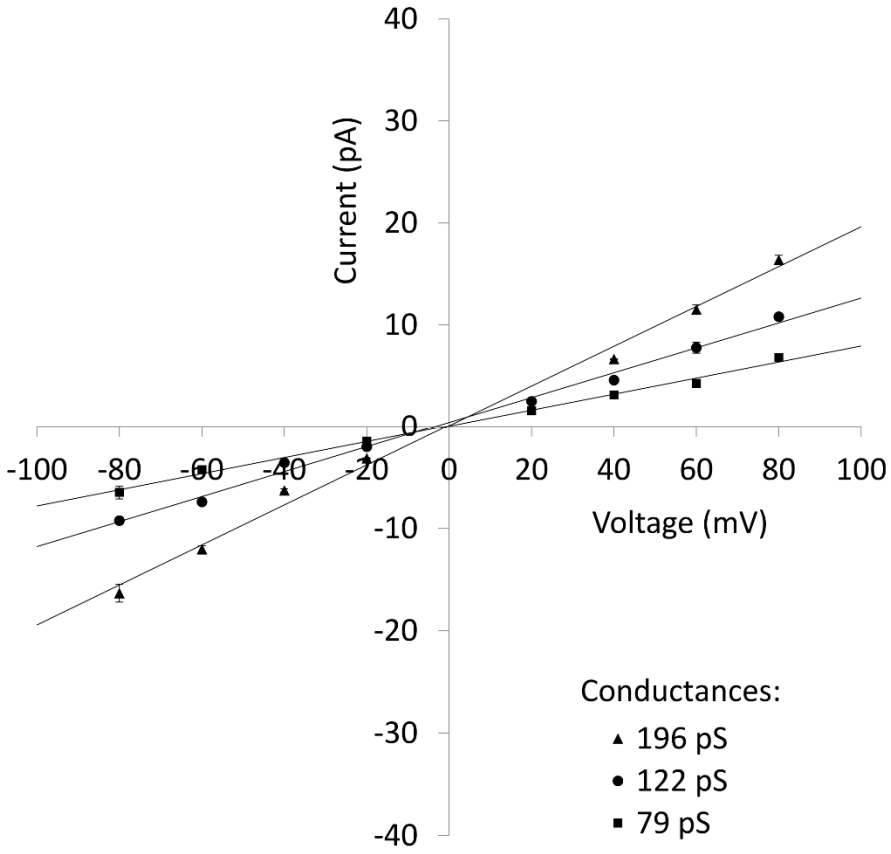

625

626 **Figure 13 Single-channel current - voltage relationship recorded in planar lipid bilayers in the presence of Cry41Aa.**

627 Current-voltage relationships (I-V curves) of single-channel activity of Cry41Aa (8 µg/ml) in a typical PLB experiment,
628 representative of three independent experiments, performed under identical symmetrical (150 mM:150 mM KCl cis/trans)
629 conditions. The data points could be fitted by three linear regressions (shown by ●, ■, and ▲ symbols) passing through the
630 origin of the I and V axes. The calculated slopes of these regression lines represent the conductances of the three most
631 common conducting states or substates of the channels formed by the toxin. In this particular experiment, they were equal to
632 79 pS (■), 122 pS (●) and 196 pS (▲).

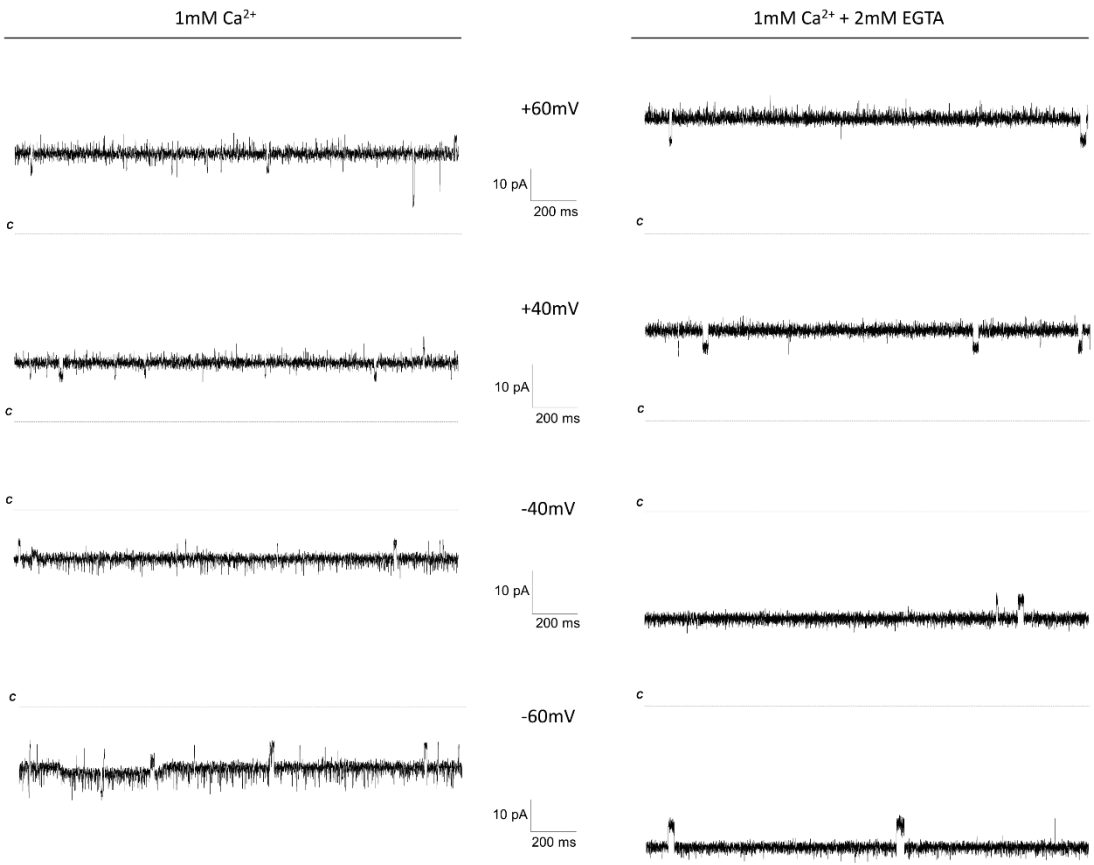

Figure 14 Cry41Aa induced channel formation in planar lipid bilayers in the presence or absence of EGTA.

Representative single-channel current traces of Cry41Aa (8 µg/ml) were recorded in planar lipid bilayer at various voltages in the presence or absence of 2 mM EGTA under symmetrical (150 mM:150 mM KCl) conditions. Traces were filtered at 1 kHz.

Ions	DMEM	Ca^{2+}-free DMEM	Advanced DMEM	DPBS	Patch-clamp buffer	PLB buffer	EGTA-metal absolute stability constant
Ca^{2+}	1.8	-	1.8	-	1.1	1	11
Mg^{2+}	0.8	0.8	0.8	-	1.1		5.2
Fe^{3+}	2.4E-4	2.4E-4	2.4E-4	-	-	-	20.5
Fe^{2+}	-	-	-	-	-	-	11.9
Mn^{2+}	-	-	3.9E-7	-	-	-	12.3
Zn^{2+}	-	-	-	-	-	-	14.5
Cu^{2+}	-	-	7.8E-6	-	-	-	17.8

Table 1 Levels of main divalent metal ions in cell media used and EGTA-metal stability constants.

Amounts (mM) of metal cations present in cell culture media were obtained from the supplier's website (www.thermofisher.com/uk/en/home.html). All culture media had pH 7.4. The table does not take into account cations present in FCS. EGTA-metal stability constants were taken from Cheng, et al. (42).

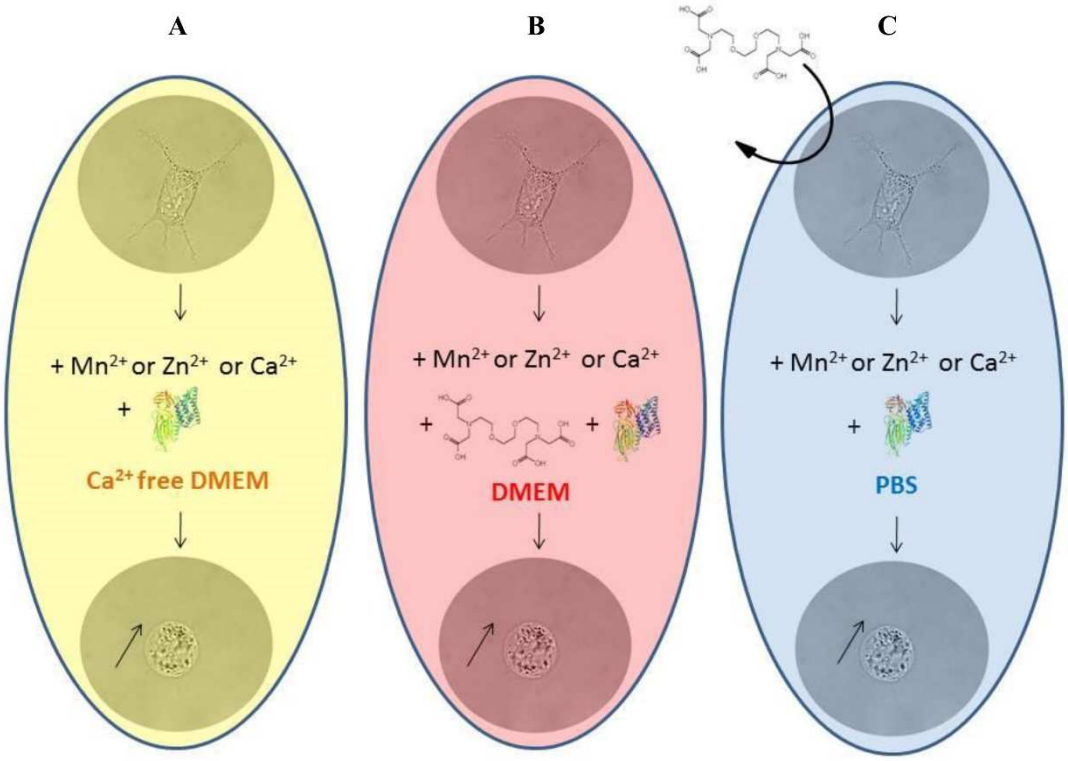

644

645 **Figure 15 Experimental evidence for the role of Zn^{2+}, Ca^{2+} and Mn^{2+} in Cry41Aa toxicity.**

646 Graphic representation of experimental design and results involving salt supplementation. (A) Zn^{2+}, Ca^{2+} and Mn^{2+} enhanced
647 Cry41Aa toxicity in Ca^{2+}-free medium. (B) Restored toxin activity after EGTA treatment in complete medium. (C)
648 Facilitated Cry41Aa toxicity in DPBS after transient EGTA treatment.

Highlights:

- EGTA, EDTA, BAPTA and DTPA chelators protect HepG2 cells from Cry41Aa cytotoxicity.
- EGTA removes membrane bound cations preventing toxin binding and membrane damage.
- Cry41Aa induces pore formation in planar lipid bilayers, also in EGTA's presence.
- Ca^{2+}, Mn^{2+} and Zn^{2+} reinstated cytotoxicity in salt supplementation assays.
- Toxin's action is dependent on interaction with metal cation-dependent receptor(s).

Ethical Statement

Hereby, I Barbara Domanska consciously assure that for the manuscript: The role of membrane-bound metal ions in toxicity of a human cancer cell-active pore-forming toxin Cry41Aa from *Bacillus thuringiensis* the following is fulfilled:

1) This material is the authors' own original work, which has not been previously published elsewhere.

2) The paper is not currently being considered for publication elsewhere.

3) The paper reflects the authors' own research and analysis in a truthful and complete manner.

4) The paper properly credits the meaningful contributions of co-authors and co-researchers.

5) The results are appropriately placed in the context of prior and existing research.

6) All sources used are properly disclosed.

7) All authors have been personally and actively involved in substantial work leading to the paper, and will take public responsibility for its content.

Date: 05/02/2019

Corresponding author's signature: